# Comparative and Structural Analysis of the Interaction between β-Lactoglobulin type A and B with a New Anticancer Component (2,2'-Bipyridin *n*-Hexyl Dithiocarbamato Pd(II) Nitrate)

A. Divsalar, A. A. Saboury,[*] H. Mansoori-Torshizi,[†] and B. Hemmatinejad[‡]

*Institute of Biochemistry and Biophysics, University of Tehran, Tehran, Iran. [*]E-mail: Saboury@ut.ac.ir*
*[†]Department of Chemistry, University of Sistan & Bluchestan, Zahedan, Iran*
*[‡]Department of Chemistry, Shiraz University, Shiraz, Iran*

The interaction between whey carrier protein β-lactoglobulin type A and B (BLG-A and -B) and 2,2'-bipyridin *n*-hexyl dithiocarbamato Pd(II) nitrate (BPHDC-Pd(II)), a new heavy metal complex designed for anticancer property, was investigated by fluorescence spectroscopy combined with chemometry and circular dichroism (CD) techniques. A strong fluorescence quenching reaction of BPHDC-Pd(II) to BLG-A and -B was observed. Hence, BPHDC-Pd(II) complex can be bound to both BLG-A and -B, and quench the fluorescence spectra of the proteins. The quenching constant was determined using the modified Stern-Volmer equation. The binding parameters were evaluated by fluorescence quenching method. The results of binding study provided evidences presence of two and three sets of binding sites on the BLG-B and -A, respectively, for BPHDC-Pd(II) complex. Using fluorescence spectroscopy and chemometry, the ability of BLG-A and -B to form an intermediate upon interaction with BPHDC-Pd(II) complex was assessed. CD studies displayed that under influence of different concentrations of BPHDC-Pd(II) complex, the regular secondary structure of BLG-B had no significant changes, whereas for BLG-A a transition from α-helix to β-structure was appeared. The results for both of BLG-A and -B displayed that BPHDC-Pd(II) complex can induce a conformational transition from the native form to an intermediate state with a slightly opened conformation, which is detectable with chemometry analyses.

**Key Words :** β-Lactoglobulin, Pd(II) complex, Chemometry analyses, Fluorescence quenching, Binding site

## Introduction

β-lactoglobulin (BLG), the major bovine whey protein, is a well-characterized globular protein and it is at present purified at industrial-scale due to its functional properties in food applications.[1] BLG, an 18 kDa polypeptide, has been identified as a member of the lipocalin super family of transporter molecules for small hydrophobic ligands.[2] This protein exists mainly as a dimmer at neutral pH. Native BLG has two disulphide bonds and one free thiol group, which is buried within the protein structure.[3] The crystal structure of bovine BLG has been determined and shows that the 162 amino acids long single polypeptide chain of BLG forms a calyx composed of an eight-stranded antiparallel β-sheet[4] in which several physiologically relevant ligands, steroids, retinoids and fatty acids were found to bind.[5-7] BLG can thus serve as a potential carrier protein especially in the case of hydrophobic compounds which can not be dissolved in aqueous solution.[5] This protein shows significant stability in solution, to the extent of being unaffected by the pH of human stomach acid. Modifications of pH can, of course, alter the conformation of BLG, as has been observed experimentally. However, these modifications do not lead to the complete denaturation of the BLG.[8] BLG exists in several genetic variants, but variant A and B are predominant. Variant A (BLG-A) differs in amino acid sequence from

variant B (BLG-B) at positions 64 (Asp$_A$ → Gly$_B$) and 118 (Val$_A$ → Ala$_B$).[9] These differences result in distinct biophysical and biochemical properties of the variants, such as heat stability, self association properties and solubility.[8-10]

Platinum drugs have played a key role among the metal-based anticancer agents. The initial discovery in 1969 of the anti-tumor properties of *cis*-platin by Rosenberg[11] was suddenly followed clinical trials demonstrating its efficacy toward a variety of solid tumors. Nowadays, *cis*-platin is one of the most reliable anticancer drugs in the treatment of a wide range of malignancies including ovarian, testicular carcinomas, lung, urinary bladder, osteosarcoma, head and neck tumors.[12,13] However, *cis*-platin and its analogues produces served side effects including, nephrotoxicity and neurotoxicity.[12] For platinum based-drugs, the predominant binding sites are the N7 and N3 atoms of the DNA bases guanine (G) and adenine (A), respectively. The N7 guanine atom lies in the DNA major groove, making it more exposed and more easily accessible, as a consequence, it represents the preferred.[12] Because Palladium chemistry is similar to that of platinum, it was speculated that Pd complexes may also exhibit anti-tumor activities. Attempts have been made to synthesis Pd(II) complexes with such activities.[14] Reports have shown that benzyl bis(thio semicarbazone) Palladium (II) complex is very effective in inhibiting proliferation in several sensitive tumor cell lines (Hela, Vero and Pam212).[15]
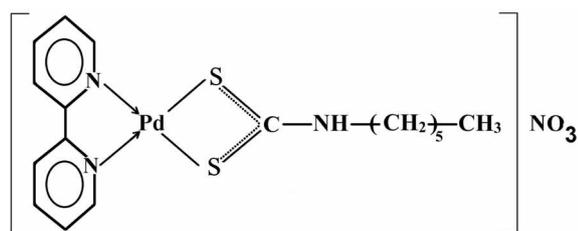
**Figure 1.** The molecular structure of BPHDC-Pd(II) complex.

Genova *et al.* have shown that Pd(II) complexes exhibit a significant activity against acyclovir-resistant viruses R-100 (HSV-1) and PU (HSV-2).[16]

The search for Palladium(II) complexes having fewer side effects is still continuing. The 2,2'-bipyridin *n*-hexyl dithiocarbamato Pd(II) nitrate (BPHDC-Pd(II)) is a novel Palladium(II) complex, which was synthesized in our group for anticancer purpose. The molecular structure of this Pd(II) complex is shown in Figure 1. In the present study, it was aimed to investigate the physical interactions between the novel designed Palladium(II) complex and the whey carrier proteins, BLG-A and -B, by fluorescence, circular dichroism and chemometry. The thermodynamic parameters obtaining from the binding studies of the Pd(II) complex to BLG as a carrier protein may be useful to evaluate the structural inducing effects of the ligand on the protein structure as the ligand side effect.

## Materials and Methods

**Materials.** Bovine BLG-A and -B were obtained from Sigma. Pd complex (2,2'-bipyridin n-hexyl dithiocarbamato Pd(II) nitrate) was synthesized in our laboratory.[17,18] All other materials and reagents were of analytical grade, and solutions were made using double-distilled water. Since BPHDC-Pd(II) complex have low solubility in buffer solutions, then it was solved in NaCl solution, 50 mM, with pH = 7.0. Concentrations of BLG-A and -B were determined spectrophotometrically, using a molecular absorption coefficient of $\varepsilon_{278\,nm} = 17,600\ M^{-1}\ cm^{-1}$.[19]

**Methods**

**Fluorescence Measurements.** Fluorescence intensity measurements were carried out on a Hitachi spectro-fluorimeter model MPF-4. The excitation wavelength was adjusted at 290 nm and the emission spectra were recorded for all of the samples in the range of 300-500 nm, using a 1-cm path length fluorescence cuvette. Samples of 7 $\mu$M BLG-A and -B were made in 50 mM NaCl solution.

**Circular Dichroism (CD) Measurements.** CD spectra were recorded on an Aviv Spectropolarimeter model 215 (Proterion Corp., USA). Changes in the secondary structures of BLG-A and -B were monitored in the far UV region (190-260 nm) using 1-mm path length cells. The protein concentration in the experiments for far UV region was 13.5 $\mu$M. The results were expressed in molar ellipticity [$\theta$] (deg cm$^2$ dmol$^{-1}$) based on a mean amino acid residue weight of 114 (MRW).[20] The molar ellipticity was determined as [$\theta$]$_\lambda$

= (100 × MRW × $\theta_{obs}$/cl), where $\theta_{obs}$ is the observed ellipticity in degrees at a given wavelength, c is the protein concentration in mg/mL and L is the length of the light path in cm. The CD software was used to predict the secondary structure of the protein according to the statistical method.[21,22]

**Chemometric Analysis.** For each system under study, the absorbance data were digitized in the 0.5 nm intervals and gathered in a ($m \times n$) data matrix **D** where $m$ and $n$ are the number of titration steps and number of wavelength, respectively. Thus, each row of matrix **D** was a digitized spectrum in an individual titration step (*i.e.* the amounts of added BPHDC-Pd(II)). This data matrix was then subjected to factor analysis[23] to evaluate the number of components. For this purpose, the data matrix was decomposed to row and column matrices by singular value decomposition (SVD) as

$$\mathbf{D = TP} \tag{1}$$

Where **T** and **P** contain the orthogonal eigen vectors spanning the row and column spaces of the original data set, respectively. Some different methods, such as real error (RE), imbedded error (IM), chi value ($\chi$), and indicator function are available for determining the number of factors.[23] The MCR-ALS subroutine written by Tauler was used to resolve the components of pure spectra and their corresponding concentration profiles. The ALS program was downloaded from the site: http://www.ub.es/gesq/mcr/mcr.htm

Here, the MCR-ALS analysis decomposes the data matrix **D** into a matrix **C** of the pure concentration profile, and a matrix **S** of pure spectral profile, related to different species of iodine in the solvent system:

$$\mathbf{D = CS + E} \tag{2}$$

In an iterative procedure, **C** and **S** are calculated so that the **CS** product constructs the original data matrix **D** with the optimal fit (*i.e.*, at a minimal residual error, **E**) based on the two following matrix equations:

$$\mathbf{C = DS^+} \tag{3}$$
$$\mathbf{S = C^+D} \tag{4}$$

The superscript '+' denotes the pseudo-inverse of a matrix. An initial guess of the concentration profile or pure spectra is needed to start the ALS optimization. Here, the evolving-factor analysis (EFA) was used to obtain the first estimate of the concentration profiles of the components. In each iterative cycle of optimization, some constraints were applied. The non-negativity, unimodality, and closure constraints were used for concentration of the profiles, and non-negativity was applied to the spectral profiles. For more information about MCR-ALS, one may refer to the papers by Diaz-Cruz *et al.*[24]

## Results

For macromolecules, fluorescence measurements can give some information on the binding of small molecule sub-
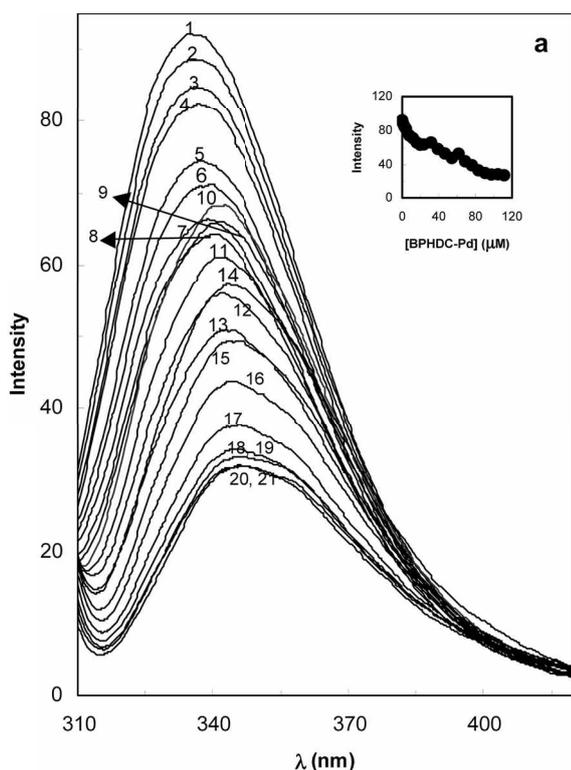
**Figure 2a.** Fluorescence spectra of BLG-A in the absence (1) and in the presence of different concentrations of BPHDC-Pd(II) complex including 0 (1), 0.8 (2), 2.4 (3), 4 (4) 8 (5), 11.9 (6), 31.4 (7), 15.8 (8), 19.7 (9), 23.6 (10), 39 (11), 46.6 (12), 54.1(13), 69 (14), 76.2 (15), 83.4 (16), 83.4 (17), 90.6 (18), 97.6 (19), 104.7 (20) and 111.6 (21) *μ*M in 50 mM NaCl solution at 27 °C. The concentration of the protein was 7 *μ*M. The inset shows the changes of the intrinsic Trp emission of the BLG-A at 335 nm upon titration with different concentrations of BPHDC-Pd(II).



**Figure 2b.** Fluorescence spectra of BLG-B in the absence (1) and in the presence of different concentrations of BPHDC-Pd(II) complex including 0 (1), 0.8 (2), 2.4 (3), 4 (4) 8 (5), 11.9 (6), 31.4 (7), 15.8 (8), 19.7 (9), 23.6 (10), 39 (11), 46.6 (12), 54.1(13), 69 (14), 76.2 (15), 83.4 (16), 83.4 (17), 90.6 (18), 97.6 (19), 104.7 (20) *μ*M in 50 mM NaCl solution at 27 °C. The concentration of the protein was 7 *μ*M. The inset shows the changes of the intrinsic Trp emission of the BLG-B at 335 nm upon titration with different concentrations of BPHDC-Pd(II).

stances to proteins, such as the binding mechanism, binding mode, binding constants, binding sites, intermolecular distances, etc.[25] The fluorescence intensity of a compound can be decreased by a variety of molecular interactions including excited-state reactions, molecular rearrangements, energy transfer, ground state complex formation and collisional quenching. Such decrease in intensity is called quenching.[26,27] The role of fluorescence quenching can be studied experimentally by determining quenching rate parameters using Stern-Volmer plots.[27] In order to investigate the binding of BPHDC-Pd(II) complex to BLG-A and -B, the fluorescence spectra were recorded in the range of 300-420 nm upon excitation at 290 nm. In order to examine fluorescence emission of BPHDC-Pd(II) complex, the emission of this complex was investigated at the highest concentration (100 *μ*M) and this complex had negligible fluorescence emission. The fluorescence intensity of BLG-A and -B decreases in the presence of BPHDC-Pd(II) complex (Fig. 2a and b) and a red shift was observed in a maximum emission wavelength ($λ_{max}$), which is probably owing to the loss of the compact structure of hydrophobic region where Trp residues are placed.[26,28] The insets show the changes of

the intrinsic Trp emission of the BLG-A and -B at 335 nm upon titration with different concentrations of BPHDC-Pd(II). Thus the fluorescence spectra were strongly quenched, whereas $λ_{max}$ was increased from 335 to 347 nm by addition of BPHDC-Pd(II) for BLG-A and -B. In order to speculate the fluorescence quenching mechanism, the fluorescence quenching data for BLG-A and -B were firstly analyzed using the classical Stern-Volmer equation:

$$\frac{F_0}{F} = 1 + K_{SV}[Q] \qquad (5)$$

Where $F_0$ and $F$ are the fluorescence intensities of BLG-A and -B in the absence and in the presence of BPHDC-Pd(II) complex, respectively. $K_{SV}$ is the Stern-Volmer dynamic quenching constant and [Q] is the total concentration of quencher (BPHDC-Pd(II)). The plots of $F_0/F$ versus [Q] showed positive deviation (Fig. 3a and b). These results indicate that the probable quenching mechanism of a BPHDC-Pd(II)-BLG-A and -B binding reactions are initiated by compound formation rather by dynamic collision. Therefore, the quenching data were analyzed according to the modified Stern-Volmer equation:[26,28]
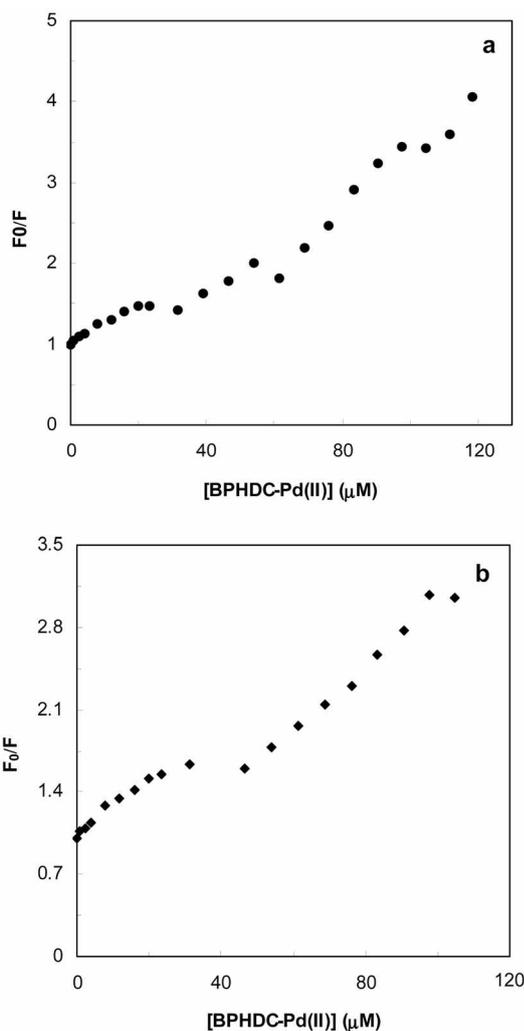
**Figure 3.** (a) The Stern-Volmer curve for quenching of BPHDC-Pd(II) complex to BLG-A in 50 mM NaCl solution at 27 °C. (b) The Stern-Volmer curve for quenching of BPHDC-Pd(II) complex to BLG-B in 50 mM NaCl solution at 27 °C.

$$\frac{F_0}{(F_0 - F)} = \frac{1}{f_a} + \frac{1}{f_a K_{S.V}} \cdot \frac{1}{[Q]} \qquad (6)$$

Where $f_a$ is the fraction of the initial fluorescence, which is accessible to quencher. The value of $f_a$ refers to the fraction of fluorescence accessible to quenching, which need not be the same as the fraction of tryptophan residue, accessible to quenching.[28] The dependence of $F_0/(F_0-F)$ on the reciprocal value of the quencher concentration (1/[BPHDC-Pd(II)]) is linear. The values of $f_a$ and $K_{S.V}$ were obtained from the values of intercept and slope, respectively (Fig. 4a and b). The values of $f_a$ for BLG-A and -B were found to be 1.82 and 1.73 indicating that 55% and 58% of the total fluorescence of BLG-A and -B were accessible to quencher, respectively. The Stern-Volmer quenching constant were calculated and listed in Table 1.

For static quenching, the following equation was employed to calculate the binding constant, $K_A$, and the number of binding sites, n:[29]
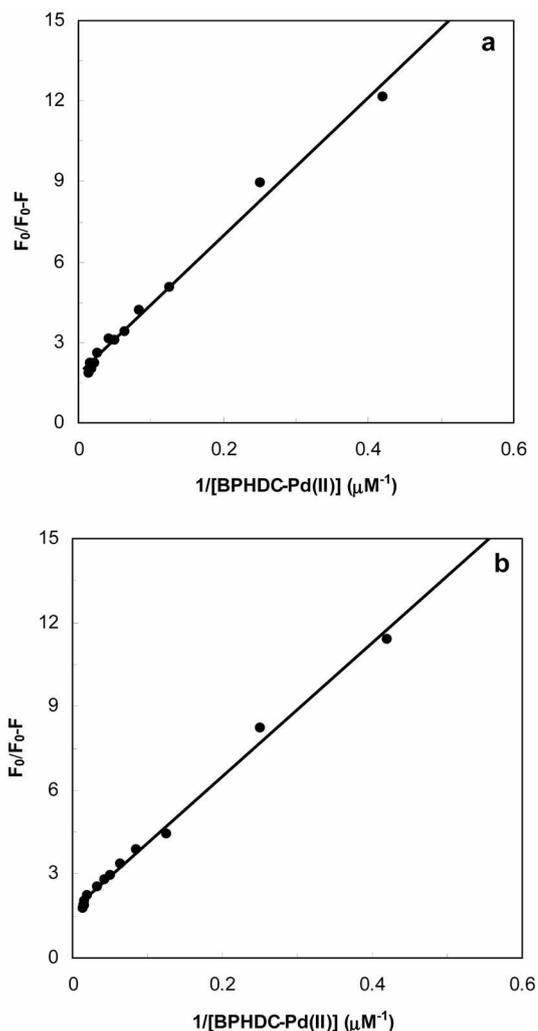


**Figure 4.** (a) The modified Stern-Volmer curve for the binding of BPHDC-Pd(II) complex to BLG-A in 50 mM NaCl solution at 27 °C. (b) The modified Stern-Volmer curve for the binding of BPHDC-Pd(II) complex to BLG-A in 50 mM NaCl solution at 27 °C.

**Table 1.** The Stern-Volmer constant ($K_{S.V}$), the fraction of the initial fluorescence, which is accessible to quencher ($f_a$), the apparent association constant ($K_A$), the number of binding sits (n) of BLG-A and -B upon interaction with BPHDC-Pd(II) complex

| Parameters | BLG-A | BLG-B |
|---|---|---|
| $K_{S.V} \times 10^3$ $(\mu M)^{-1}$ | 70.4 | 72.3 |
| $f_a$ | 0.53 | 0.58 |
| First binding set: | | |
| $K_A$ (nm$^{-1}$) | 11.1 | 10 |
| n | 10 | 13.5 |
| Second binding set: | | |
| $K_A$ (nm$^{-1}$) | 25.1 | 60 |
| n | 5 | 14.3 |
| Third binding set: | | |
| $K_A$ (nm$^{-1}$) | 27.3 | – |
| n | 2.5 | – |

$$\frac{F_0}{F} = K_A \frac{[Q]F_0}{F_0 - F} - n K_A [P]_t \qquad (7)$$
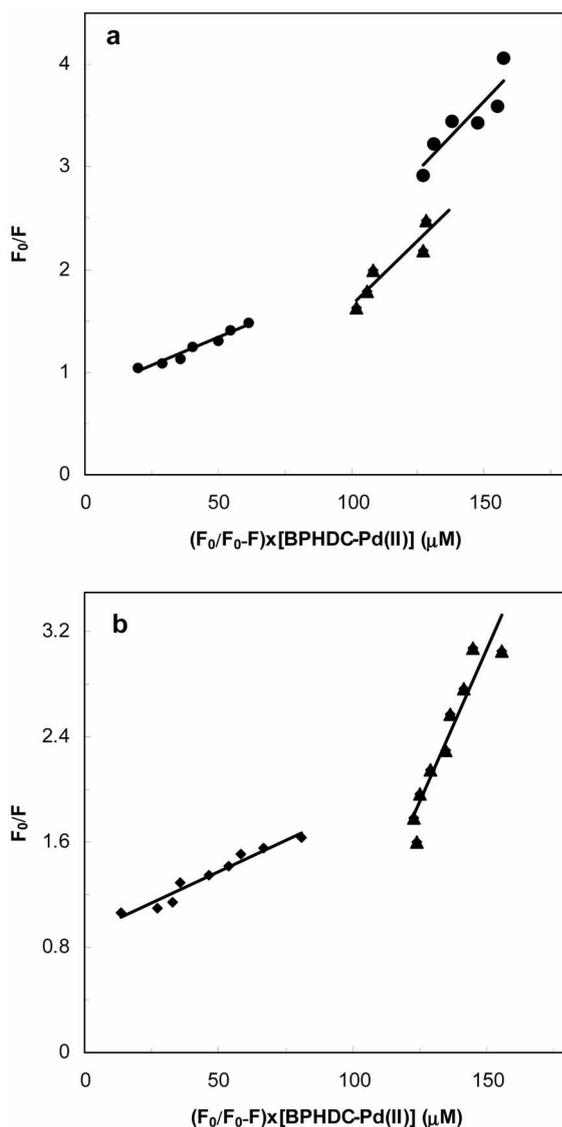
**Figure 5.** (a) The best linear plot of $F_0/F$ versus $[Q] \times (F_0/F_0-F)$ according to the equation (7). Values of $K_A$ and n for binding of BPHDC-Pd(II) complex to BLG-A can be obtained from the slope and the vertical-intercepts, respectively. (b) The best linear plot of $F_0/F$ versus $[Q] \times (F_0/F_0 - F)$ according to the equation (7). Values of $K_A$ and n of binding of BPHDC-Pd(II) complex to BLG-B can be obtained from the slope and the vertical-intercepts, respectively



**Figure 6.** (a) Mole fraction of components (MFC) present in BLG-A-BPHDC-Pd(II) complex solution versus BPHDC-Pd(II) complex concentration. The sympols of (I), (N) and (D) present the intermediate, Native and denatured state of BLG-A in the presence of BPHDC-Pd(II) complex. (b) Mole fraction of components (MFC) present in BLG-B-BPHDC-Pd(II) complex solution versus BPHDC-Pd(II) complex concentration. The sympols of (I), (N) and (D) present the intermediate, Native and denatured state of BLG-B in the presence of BPHDC-Pd(II) complex.

Where $F_0$ and $F$ are the fluorescence intensities of BLG-A and -B in the absence and presence of quencher (BPHDC-Pd(II)), $K_A$ is the apparent association constant for the equilibrium formation of BLG-Pd(II) complex and $[Q]$ and $[P]_t$ are the total concentration of quencher (BPHDC-Pd(II) complex) and proteins (BLG-A and -B), respectively. Thus, a plot of $F_0/F$ versus $[Q] F_0/(F_0-F)$ can be used to determine $K_A$ as well as n. As shown in Figure 5a and b, BPHDC-Pd complex can bind in three sets of binding sites on the BLG-A, but it can bind in two sets of binding sites on the BLG-B. The binding data ($K_A$ and n) for BLG-A and -B presented in Figure 5 have been given in Table 1.

The fluorescence spectra obtained in the previous section,

were the crude data for chemometric analysis to determine the number of total compounds present in the solution and their mole fraction in different steps of interaction, which are shown in Figure 6a and b as the mole fraction of compounds (MFC) versus BPHDC-Pd(II) complex concentration. From these concentration profiles, it is seen that in the presence of BPHDC-Pd complex, the distribution of intermediates and their mole fraction of BLG-A and -B are altered, which result binding of this complex and changing the tertiary structure of the both proteins (Figures 2 and 4).

CD has proved to be an ideal technique for monitoring conformational changes in proteins, which can occur as a result of changes in experimental parameters such as pH, temperature, binding of ligands and so on.[30] The far UV-CD spectra characterize the secondary structure of proteins due

**Table 2.** Content of the secondary structure of BLG-A upon interaction with BPHDC-Pd(II) complex in different concentrations

| [BPHDC-Pd(II)] (μM) | % α-Helix | % β-Sheet | % Random coil |
|---|---|---|---|
| 0 | 17.4 | 42.6 | 40 |
| 15.4 | 17.3 | 42.5 | 40.2 |
| 45.8 | 16.9 | 43.3 | 39.8 |
| 61.6 | 14.6 | 45 | 40.4 |
| 123.1 | 13.5 | 47.4 | 39.1 |
| 169.3 | 11.9 | 48.9 | 39.2 |
| 215.3 | 10.9 | 50 | 39.1 |

**Table 3.** Content of the secondary structure of BLG-B upon interaction with BPHDC-Pd(II) complex in different concentrations

| [BPHDC-Pd(II)] (μM) | % α-Helix | % β-Sheet | % Random coil |
|---|---|---|---|
| 0 | 17.8 | 44 | 38.2 |
| 15.4 | 20.1 | 41.9 | 38 |
| 45.8 | 17.3 | 44.3 | 38.4 |
| 61.6 | 18.3 | 43.7 | 38 |
| 123.1 | 18.2 | 43.9 | 37.9 |
| 169.3 | 18 | 44 | 38 |
| 215.3 | 18 | 44.3 | 37.7 |

μM for BLG-A, the content of regular secondary structure of the protein does not show any significant change. But in the presence of the concentrations of 61.6 μM up to 215.3 μM (equal to the point of starting of the second set of binding sites up to filling of the third binding set) the content of α-helix decreases (Table 2). Tables 2 and 3 show the content of the secondary structure of BLG-A and -B upon interaction with BPHDC-Pd(II) complex in different concentrations. As shown in Table 2, decreasing in the of α-helix content of BLG-A compensates with an increase in the content of β-sheet. Then, it can be concluded that in the presence of the high concentrations of BPHDC-Pd(II) complex, the β-sheet structure can induce in the secondary structure of BLG-A. As it is shown in Figure 7b the content of regular secondary structures of the BLG-B does not show any alteration in the presence of the different concentrations of BPHDC-Pd(II) (Table 3).

**Figure 7.** (a) Far-UV circular dichroism spectra of 13.5 μM BLG-A measured in the absence (a) and presence of different concentrations of BPHDC-Pd(II) complex: 15.4 (b), 45.8 (c), 61.6 (d), 123.1 (e), 169.3 (f) and 215.3 (g) μM in 100 mM NaCl solution at 27 °C. (b) Far-UV circular dichroism spectra of 13.5 μM BLG-B measured in the absence (a) and presence of different concentrations of BPHDC-Pd(II) complex: 15.4 (b), 45.8 (c), 61.6 (d), 123.1 (e), 169.3 (f) and 215.3 (g) μM in 100 mM NaCl solution at 27 °C.

**Discussion and Conclusion**

It is observed that in the both types of BLG (A and B), the Stern-Volmer plots are nonlinear, showing positive deviation (Fig. 3a and b). Also similar experimental results observed by others.[32,33] From the Stern-Volmer plot, it may be concluded that the quenching is not collisional and may be due to the formation of either the ground state complex or static quenching process.[33,34] The BLG intrinsic fluorescence is due to the two Trp residues in the position 19 and 61. According the structural models, the indole group of Trp-19 is located inside the calyx of the protein while Trp-61 is a part of an external loop and close to the cysteines 160-66

to the peptide bond absorption.[31] The CD spectrum of BLG is typical of a protein that is composed of antiparallel β-structure and shows a minimum at 217 nm.[30] The far UV-CD spectrum of BLG-A and -B in the absence and in the presence of different concentrations of BPHDC-Pd(II) complex (0, 15.4, 45.8, 61.6, 123.1, 169.3 and 215.3 μM) are shown in Figure 7a and b, respectively. Fig. 7a shows that addition of BPHDC-Pd(II) up to concentration of 45.8

disulfide bond. The water accessibility to Trp-19 is, accordingly, much lower than Trp-61.[4,31,35,36] Cho *et al.* genetically modified Trp-19 to Ala-19 and showed that the intrinsic fluorescence was substantially diminished, demonstrating that Trp-61 was a minor contributor to overall fluorescence emission.[37] This can be due to the location of Trp-61 near a disulfide bond (Cys 66-160) or near the guanidine group of Arg-124 (3-4 Å distance from Trp-19 indole ring,[38] which can quench its emission and/or to the self-quenching of Trp-61 of the other monomer in the BLG dimeric form.[31,35] From the intercept values of $f_a$, it can be concluded that about 55% and 58% (for BLG-A and -B, respectively) of the tryptophanyl fluorescence are accessible for quenching by BPHDC-Pd(II), and the others 45% and 42% (for BLG-A and -B, respectively) are not affected by BPHDC-Pd(II) (Fig. 3a and b). Further information regarding the environment of the accessible Trp side chains can be obtained from the fluorescence spectra, since the wavelength at maximum fluorescence of the indole fluorophore depends upon solvent polarity. The red shift observed, 12 nm, (Fig. 2a and b) shows that side chains exposed to the polar aqueous environment. Studies on tryptophyl model compounds have shown that the interaction between their excited states and the polar solvent causes a red shift of the fluorescence spectrum.[39] Then, the location of $\lambda_{max}$ of the difference spectrum at 347 nm shows that these accessible tryptophyls are largely exposed to the aqueous solvent.[39] Also, the position of the emission maximum of the native BLG at 335 nm, is not characteristic of a completely non polar medium, suggesting some contribution to the spectrum of the more surface exposed Trp-61. The observation of the red shift, by the increasing of the BPHDC-Pd(II) complex concentrations (Fig. 2a and b) might be due to a non polar Trp environment than in the native state, this might indeed happen with Trp-19 if the calyx structure of BLG has partially loosened.[28,31] Alternatively, a red shift might be due to the increased contribution of Trp-61 (which has a more red shifted emission than Trp-19) to the fluorescence spectra.

Binding studies show that the values of the $K_A$ corresponding to the first binding set up to the third binding set from 11.1 to 27.3 nm$^{-1}$ in BLG-A and the values related to the first binding set up to second binding set in BLG-B from 10 to 60 nm$^{-1}$ increased. Increasing of the $K_A$ values indicated the increasing of the affinity of the proteins to BPHDC-Pd(II) complex. From above results, it can be concluded that by the binding of the BPHDC-Pd(II) complex into the first binding set, the tertiary structure of the protein changed, then the latter binding sets with higher affinity appeared. These findings have a good agreement with fluorescence studies that show a slightly opened tertiary structure of the protein related to the observation of red shift in $\lambda_{max}$.

By the aid fluorescence spectroscopy and chemometry, we could detect the ability of BLG-A and -B to form intermediates upon interaction with BPHDC-Pd(II) complex. On the other hand, it can be seen that BPHDC-Pd(II) complex induced slightly opened conformation on the tertiary structure of BLG-A and -B, then the native state of the protein changed to the intermediate state that detected by chemometry analyses.

Studies on the Pd complexes have shown that these complexes bind to the heteroatoms in the side chain of Met or His and promote cleavage of the amide bond involving the carboxylic group of this anchoring amino acid.[40] Zhu *et al.*[41] showed that Pd complexes have two sites for binding that each site of major cleavage is a peptide bond followed by two residues, the first of which is Serine (Ser) or Threonine (Thr) and the second one is Histidine (His) or Meteonine (Met).[41-45] The binding studies indicate that BLG-A has three binding sets for BPHDC-Pd(II), which first binding set including 10 binding sites. By determining of the surface accessible amino acids of the protein,[46,47] It is expected that the first binding set might be filled by four surfaces accessible Ser(s) (30 and 36 from both monomers) and six Thr(s) (154, 125 and 18 from both monomers). After the filling of the first binding set, the structure of the protein slightly unfolds (due to the 12 nm red shift in fluorescence spectra), then the latter sets fill by the His (146 from both monomers) and Met(s) (7, 145, 107 and 24 from both monomers) that expose to the surface of the protein.

Binding of BPHDC-Pd(II) complex induces one intermediate state in the structure of both BLG-A and -B. The intermediate state of hydrophobic molecule-binding proteins, including BLG, may have some physiological significance and may be related to the functional release of retinal or other hydrophobic compounds bound to the proteins.[48] Since a transition from α-helix to β-structure in BLG-A was seen upon interaction with BPHDC-Pd(II) complex, it may be considered as a deleterious effect of the designed ligand on the protein structure. Transition from α to β-structure appears to be physiologically important. It has been reported that the conformational switch from the α-helix to β-sheet leading to formation of amyloid structures.[49] Also the α-helix to β-sheet conformational transition(s) has been shown successfully in Alzheimer's AB peptide.[49] Different sequences of two variants of A and B by two amino acids lead to different observations in their binding properties. The result obtaining from the interaction of BPHDC-Pd(II) with whey carrier proteins probably provide useful information to design better metal anticancer complexes with lower side effects in the future.

## References

1. Relkin, P. *Int. J. Biol. Macrol.* **1998**, *22*, 59.
2. Lange, D. C.; Kotari, R.; Ramesh, P. C.; Shutish, P. C. *Biophys. Chem.* **1998**, *74*, 45.
3. Hong, Y. H.; Creamer, L. K. *Int. Dairy J.* **2002**, *12*, 345.
4. Sawyer, L.; Kontopidis, G. *Biochim. Biopys. Acta* **2000**, *1482*, 136.
5. Jankowski, C. K.; Sichel, D. I. *J. Mol. Struct.* **2003**, *629*, 185.
6. Zsila, F.; Bikadi, Z. *Spectrochimica. Acta* **2005**, *62*, 666.
7. Busti, P.; Scarpeci, S.; Gatti, C. A.; Delorenzi, N. *J. Food.*

*Hydrocolloids* **2005**, *19*, 249.

8. Bon, C. L.; Domonique, D.; Nicolari, T. *Int. Dairy J.* **2002**, *12*, 671.

9. Oliveira, K. M. G; Valente-Mesquita, V. L.; Botelho, M. M.; Sawyer, L. *Eur. J. Biochem.* **2001**, *268*, 477.

10. Divsalar, A.; Saboury, A. A.; Moosavi-Movahedi, A. A.; Mansoori-Torshizi, H. *Int. J. Biol. Macro.* **2006**, *38*, 9.

11. Rosenberg, B.; Van Kamp, L.; Trosko, J. E.; Mansour, V. H. *Nature* **1969**, *222*, 385.

12. Giovavagnini, L.; Marzano, C.; Bettio, F.; Fregona, D. *J. Inorg. Biochem.* **2005**, *99*, 2139.

13. Budzisz, E.; Krajewska, U.; Rozalski, M. *Polish J. Pharm.* **2004**, *56*, 473.

14. Zhang, Q.; Zhong, W.; Xing, B.; Tang, W.; Chen, Y. *J. Inorg. Biochem.* **1998**, *72*, 195.

15. Matesanz, A. I.; Perenz, J. M.; Navarro, P.; Moreno, J. M.; Colacio, E.; Souza, P. *J. Inorg. Biochem.* **1999**, *76*, 29.

16. Genova, P.; Varadiniva, T.; Matesanz, A. I.; Marinova, D.; Souza, P. *Toxic. Appli. Pharm.* **2004**, *197*, 107.

17. Paul, A. K.; Mansouri-Torshizi, H.; Srivastava, T. S.; Chavan, S. J.; Chitnis, M. P. *J. Inorg. Biochem.* **1993**, *50*, 9.

18. Mansouri-Torshizi, H.; Srivastava, T. S.; Perekh, H. K.; Chitnis, M. P. *J. Inorg. Biochem.* **1992**, *45*, 135.

19. Dufour, E.; Michael, C.; Heartle, T. *FEBS Lett.* **1990**, *277*, 223.

20. Piez, K. A.; Davie, E. W.; Folx, J. E.; Gladner, J. A. *J. Biol. Chem.* **1961**, *236*, 2912.

21. Manavalan, P.; Johnson, C. J. R. *Anal. Biochem.* **1987**, *167*, 76.

22. Yang, J. T.; Wu, C. S. C.; Martinez, H. M. *Meth. Enzymol.* **1986**, *130*, 208.

23. Malinowski, E. R. *Factor Analysis in Chemistry*; Wiley & Sons: New York, 1991.

24. Diaz-Cruz, M. S.; Mendieta, J.; Tauler, R.; Esteban, M. *Anal. Chem.* **1999**, *71*, 4629.

25. Gao, H.; Lei, L.; Liu, J.; Kong, Q.; Chen, X.; Hu, Z. *J. Photochem. Photobiol. A* **2004**, *167*, 213.

26. Shaikh, S. M. T.; Seetharamappa, J.; Kandagal, P. B.; Ashoka, S. *J. Mol. Struct.* **2006**, *786*, 46.

27. Suresh Kumar, H. M.; Kunabenchi, R. S.; Biradar, J. S.; Math, N.

N.; Kadadevarmath, J. S.; Inamdar, S. R. *J. Lumin.* **2006**, *116*, 35.

28. Hu, Y.; Liu, Y.; Pi, Z.; Qu, S. S. *Bioorg. Med. Chem.* **2005**, *13*, 6609.

29. Liu, X. F.; Xia, Y. M.; Fang, Y. *J. Inorg. Biochem.* **2005**, *99*, 1449.

30. Kelly, S. M.; Price, N. C. *Curr. Protein Peptide Sci.* **2000**, *1*, 349.

31. Viseu, M. T.; Carvalho, T. I.; Costa, S. M. B. *Biophys. J.* **2004**, *86*, 2392.

32. Busti, P.; Gatti, C. A.; Delorenzi, N. J. *Int. J. Biol. Macromol.* **1998**, *23*, 143.

33. Kumar, H. M. S.; Kunabenchi, R. S.; Biradar, J. S.; Math, N. N.; Kadadevarmath, J. S.; Inamdar, S. R. *J. Lumin.* **2006**, *116*, 35.

34. Tian, F.; Johnson, K.; Lesar, A. E.; Moseley, H.; Ferguson, J.; Samuel, I. D. W.; Mazzini, A.; Brancaleon, L. *Biochim. Biophys. Acta* **2006**, *1760*, 38.

35. Creamer, L. K. *Biochemistry* **1995**, *34*, 7170.

36. Sakai, K.; Sakurai, K.; Sakai, M.; Hoshino, M.; Goto, Y. *Protein Sci.* **2000**, *9*, 1719.

37. Cho, Y.; Batt, C. A.; Sawyer, L. *J. Biol. Chem.* **1994**, *269*, 11102.

38. Brownlow, S.; Cabral, J. H. M.; Cooper, R.; Flower, D. R.; Yewdall, S. J.; Polikarpov, I.; North, A. C. T.; Sawyer, L. *Structure* **1997**, *5*, 481.

39. Leher, S. S. *Biochemistry* **1971**, *10*, 3254.

40. Djuran, M. I.; Milinkovic, S. U. *Polyhedron* **1999**, *18*, 3611.

41. Zhu, L.; Kostic, N. *Inorg. Chim. Acta* **2002**, *339*, 104.

42. Tatjana, N.; Kostic, P.; Kostic, N. *J. Am. Chem. Soc.* **1996**, *118*, 51.

43. Tatjana, N.; Kostic, P.; Kostic, N. *J. Am. Chem. Soc.* **1996**, *118*, 5946.

44. Zhu, L.; Kostic, P.; Kostic, N. *Inorg. Chem.* **1992**, *31*, 3994.

45. Zhu, L.; Kostic, P.; Kostic, N. *J. Am. Chem. Soc.* **1993**, *115*, 4566.

46. Fraczkiewicz, R.; Braun, W. *J. Comp. Chem.* **1998**, *19*, 319.

47. Divsalar, A.; Saboury, A. A.; Moosavi-Movahedi, A. A. *Protein J.* **2006**, *25*, 157.

48. Ragona, L.; Fogolari, F.; Romagnoli, S.; Zetta, L.; Maubois, J. L. *J. Mol. Biol.* **1999**, *293*, 953.

49. Bokvist1, M.; Lindstro, F.; Watts, A. *J. Mol. Biol.* **2004**, *335*, 1039.